

Quantum Control of the Hyperfine Spin of a Cs Atom Ensemble

Souma Chaudhury,¹ Seth Merkel,² Tobias Herr,¹ Andrew Silberfarb,² Ivan H. Deutsch,² and Poul S. Jessen¹

¹*College of Optical Sciences, University of Arizona, Tucson, Arizona 85721, USA*

²*Department of Physics and Astronomy, University of New Mexico, Albuquerque, New Mexico 87131, USA*

(Received 1 June 2007; published 16 October 2007)

We demonstrate quantum control of a large spin angular momentum associated with the $F = 3$ hyperfine ground state of ^{133}Cs . Time-dependent magnetic fields and a static tensor light shift are used to implement near-optimal controls and map a fiducial state to a broad range of target states, with yields in the range 0.8–0.9. Squeezed states are produced also by an adiabatic scheme that is more robust against errors. Universal control facilitates the encoding and manipulation of qubits and qudits in atomic ground states and may lead to the improvement of some precision measurements.

DOI: [10.1103/PhysRevLett.99.163002](https://doi.org/10.1103/PhysRevLett.99.163002)

PACS numbers: 32.80.Qk, 02.30.Yy, 39.25.+k, 42.50.-p

Accurate dynamical control plays a central role when quantum mechanics is leveraged to improve the outcome of a physical process. Quantum control has been accomplished in many contexts and at various levels of sophistication in areas such as nuclear magnetic resonance [1], coherent chemistry [2], quantum information processing [3], and quantum metrology [4]. One extensively studied problem is how to transfer a physical system from an initial to some final state, as is done, for example, in optical control of chemical reactions [2]. In such cases, the figure of merit for control is the yield, or fidelity [3], between the actual and the desired state. As long as errors and decoherence are negligible, the general topography of control landscapes (yield vs control parameters) is well understood [5], and techniques are available for efficient design of optimal controls [6]. The most ambitious level of quantum control requires that the system be *controllable* in the Lie-algebraic sense [7], a sufficient condition for which is that internal dynamics plus interaction with external fields can generate any unitary transformation within state space. Even when full control is possible in principle, attention must be paid to robustness in the presence of dissipation and errors in the control fields. In spin-1/2 systems, this can be accomplished by open loop control [8], i.e., without recourse to real-time feedback [9] or error correction [3], but little is known about robust controls in larger state spaces.

In this Letter, we demonstrate quantum control of the spin angular momentum (nuclear plus electronic) associated with the $F = 3$ hyperfine ground state of individual ^{133}Cs atoms, corresponding to a $(2F + 1 = 7)$ -dimensional state space. Starting from an easily prepared fiducial state, we use magnetic fields and ac Stark shifts (light shifts) to perform near-optimal control and produce a range of target states. We evaluate our control performance by reconstructing the spin density matrix [10] and computing the fidelity between the measured and the target states. In most cases, the estimated yield is in the 0.8–0.9 range, limited by errors in the control fields and to a lesser extent by decoherence from light scattering. The measured states can also be compared to a full model prediction including

errors and decoherence. Typical fidelities between measured and predicted states are around 0.9, close to the resolution limit of our state estimation procedure. We also use optimal control to produce spin-squeezed states and compare against a method based on adiabatic evolution [11] that is more robust against control errors. Large spins provide a testing ground for the design of accurate and robust controls in a system where the Hamiltonian is well known and errors and dissipation can be accurately modeled. From a practical perspective, quantum control of hyperfine states is relevant for neutral atom quantum computing [12], wherein qubits or qudits [13] are encoded in the ground-state manifold, and may provide a route to modest spin squeezing and gains in precision atomic magnetometry [14].

Universal control of a spin F requires that the Hamiltonian dynamics be capable of generating an arbitrary unitary transformation in $SU(2F + 1)$. A linear Zeeman interaction between the atomic magnetic moment and a weak magnetic field generates only Larmor precession and geometric rotations that represent $SU(2)$. More general control requires a Hamiltonian that is nonlinear in at least one component of \mathbf{F} . In our experiment, this is provided by an off-resonance light field that couples to the atomic ground state through the tensor ac polarizability and leads to a spin-dependent light shift with an irreducible rank-2 component [15]. The combination of a time-dependent magnetic field and a static x -polarized light field results in a control Hamiltonian [16]

$$H_C(t) = g_f \mu_B \mathbf{B}(t) \cdot \mathbf{F} + \kappa \hbar \gamma_s F_x^2, \quad (1)$$

where we have expressed the strength of the nonlinearity in terms of the photon scattering rate γ_s and where the dimensionless parameter κ is a measure of the time scales for coherent versus incoherent evolution. Its value depends on the atomic structure and the frequency of the driving field and for Cs takes on a maximum value $\kappa = 8.2$ when tuned between the D_1 hyperfine transitions at 894 nm. This is enough to allow considerable coherent manipulation. It follows from the theory of Lie groups that a Hamiltonian of

this form allows full control of a spin of any magnitude [17]. Specifically, one can show that the algebra generated by commutators and linear combinations of F_x , F_y , F_x^2 spans the entire $[(2F+1)^2 - 1]$ -dimensional operator space needed to represent $SU(2F+1)$. Thus, a time-varying magnetic field in the x - y plane suffices to make $H_C(t)$ universal.

A schematic of our setup for quantum control is shown in Fig. 1(a). We begin with a sample of a few million Cs atoms, laser cooled to $\sim 2 \mu\text{K}$ and initialized by optical pumping into a state of maximum projection along the y axis, $|\psi_0\rangle = |m_y = 3\rangle$. Our control magnetic field is applied by a set of low-inductance coils driven by arbitrary waveform generators, with an accuracy of better than 1% and a modulation bandwidth of more than 100 kHz. Using an all-glass vacuum cell, avoiding nearby conductive or magnetizable materials, and synchronizing our ~ 0.5 ms duration experiment to a fixed point during the ac line cycle allows us to null the background magnetic field to $\sim 100 \mu\text{G}$ without shielding or active compensation. Immediately following a period of quantum control, we estimate the resulting quantum state as described in Ref. [10]. In this procedure, the control magnetic and optical fields are applied to drive the spins for an additional 1.5 ms, while continually and weakly measuring a spin observable through its coupling to the probe polarization. To reduce the effect of noise, the measurement signal is averaged over 16 repetitions of the experiment and the density matrix determined from the measurement record and the known evolution.

Control Hamiltonians for our experiment are designed through a simple procedure that we have found to produce very good though not provably optimal results. The objective is to start from the state $|\psi_0\rangle$ and to produce a specified target state $|\chi_T\rangle$ by modulating the field $\mathbf{B}(t)$ for a fixed time τ . With readily available magnetic fields, the time scale for geometric rotations is much shorter than for nonlinear evolution driven by the light shift, and the latter

therefore becomes the time-limiting element of most transformations. In our experiment, the maximum magnetic field strength is 42 mG, corresponding to a Larmor frequency of 15 kHz, and the nonlinear strength is $\kappa\gamma_S \approx 2\pi \times 500$ Hz. Under these conditions, there is no significant sacrifice in control performance when the set of available rotations is somewhat restricted. We therefore choose the magnetic field to have constant magnitude and a time-dependent direction in the x - y plane. With this simplification, the control Hamiltonian is completely determined by the angle $\phi(t)$ between $\mathbf{B}(t)$ and the x axis. The transformation $|\psi_0\rangle \rightarrow |\chi_T\rangle$ acts in a ($d = 7$)-dimensional state space and can be specified by a set of $2d - 2 = 12$ real numbers. Full control requires at least that many free parameters in the control Hamiltonian. To ensure sufficient flexibility, we specify the control waveform $\phi(t)$ by its values $\{\phi_i\}$ at $N = 30$ discrete time steps.

The design of a control waveform proceeds through two search iterations. At first, we calculate the state $|\psi_P\rangle$ produced by a sequence of field directions $\{\phi_i\}$ by integrating the Schrödinger equation, with suitable filtering of the corresponding $\mathbf{B}(t)$ to reflect bandwidth and slew rate limitations of our magnetic coils and drivers. A locally optimal control waveform is found by starting from a random seed $\{\phi_i\}$ and maximizing the yield $\mathcal{Y} = |\langle \chi_T | \psi_P \rangle|^2$ with a gradient ascent algorithm. We have found that just a few seeds are needed to generate at least one waveform with yield ≥ 0.99 , which is expected from the general structure of control landscapes derived in Ref. [5]. At this point, we switch to a more realistic estimate of control performance, modeling the evolution with a full master equation that incorporates decoherence from light scattering and variation of the nonlinear strength across the ensemble. This allows a second stage of optimization, starting with the waveform from round one and using the complete but computationally intensive model to predict the yield, now defined in terms of the

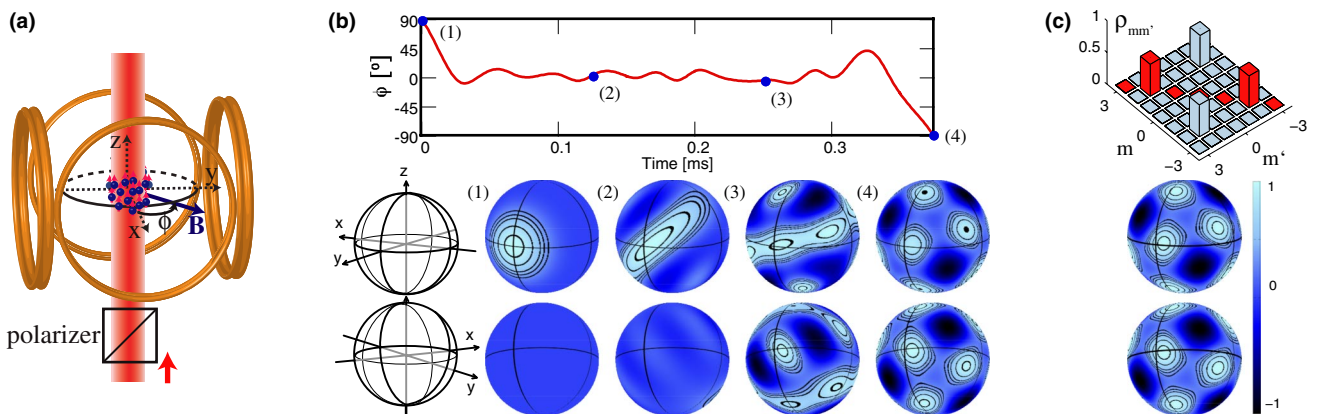


FIG. 1 (color online). Quantum control of a large atomic spin. (a) Schematic of the experiment. (b) Example of a control waveform $\phi(t)$. (1)–(4) Wigner functions calculated at four stages during the control sequence. Both sides of the sphere are shown, using two different viewpoints and a rotating frame to transform away overall rotation due to $\mathbf{B}(t)$. The final result is close to the target state $|\chi_T\rangle = (|m_z = 2\rangle + |m_z = -2\rangle)/\sqrt{2}$. (c) Density matrix (absolute values) and Wigner function for $|\chi_T\rangle$.

fidelity $\mathcal{Y} = \text{Tr}\sqrt{\rho_T^{1/2}\rho_P\rho_T^{1/2}}$ between the target (ρ_T) and the predicted (ρ_P) density matrices.

An example of an optimized control waveform is shown in Fig. 1(b), along with Wigner function representations of the spin wave packet [18] at intervals during the transformation as calculated by Schrödinger integration. Note that the nonlinear evolution initially produces a squeezing ellipsoid, which later wraps around the sphere so that interference effects can be manipulated to create the desired state. The end product is very close to the target state shown in Fig. 1(c). According to our model, this and all of our other control waveforms produce yields near 0.95. Taking into account imperfect optical pumping in our experiment (the initial population in $|\psi_0\rangle$ is ~ 0.96) reduces the expected yields to around 0.90.

We have tested a sample of control waveforms designed to produce 21 different pure spin states. Figure 2 shows three examples of target and measured density matrices, with yields in the range 0.87–0.97. A more complete statistics of yields for over a hundred experimental realizations of control is compiled as a histogram in Fig. 3(a), showing a fairly broad distribution centered on a respectable value of 0.8. It is informative to compare the measured density matrices ρ_M also against the density matrices ρ_P predicted by our model, quantified by the fidelity of control $\mathcal{F}_C = \text{Tr}\sqrt{\rho_P^{1/2}\rho_M\rho_P^{1/2}}$. Figure 3(b) shows a histogram of fidelities for our data set. Note that both yield and fidelity can be affected by control errors (the actual state is different from ρ_P) as well as state estimation errors (the actual state is different from ρ_M) and that we cannot distinguish between these possibilities. Numerical modeling shows that small background magnetic fields or miscalibration of the control fields will lead to apparent geometric rotations of the final state, but such errors are too small to be significant in our experiment. The obvious outliers in the yield and fidelity distributions are associated with two specific final states and their respective control waveforms, and closer examination shows that the measured states are

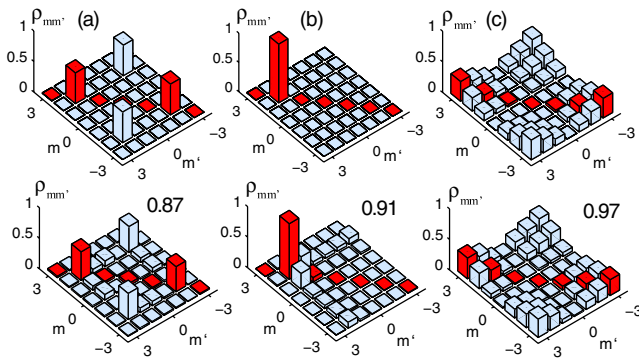


FIG. 2 (color online). Examples of target and measured density matrices (absolute values). The target states are (a) $(|m_z = 2\rangle + |m_z = -2\rangle)/\sqrt{2}$, (b) $|m_x = 2\rangle$, and (c) $\sum_y m_y |m_y\rangle$. The experimental yield is indicated for each case.

rotated with respect to the predicted states. The axis of rotation corresponds to the magnetic field direction at the transition between the control and state estimation parts of the experimental sequence, which suggests a problem with the way the corresponding control waveforms were joined together. As part of our data analysis, we can independently rotate each individual ρ_M to maximize its fidelity relative to ρ_P and obtain new values for yield and fidelity. Carrying out this procedure for all data points takes care of the outliers without otherwise changing the yield distribution significantly, as shown in Fig. 3(c). This distribution can reasonably be interpreted as a measure of our ability to control the spins in a well-designed experiment. The fidelity distribution [Fig. 3(d)] remains peaked at ~ 0.9 , which we know from experience to reflect the accuracy of our state estimation protocol. Note that random errors in state estimation are more likely to decrease than increase an apparent yield and that a better estimate of the real range of yields can be obtained if the error statistics are taken into account. As a reasonable first step, we use a simple error model, wherein the measured states undergo normally distributed random displacements in state space relative to the actual states, which in a similar way are displaced relative to the target states. This model suggests that the real yields (actual vs target state fidelity) are roughly 10% higher on average than those in Fig. 3(c). This puts most real yields in the range 0.8–0.9, in good agreement with the ~ 0.9 predicted by the model used to design the control waveforms.

To further explore quantum control in our system, we have studied the generation of spin squeezing by optimal control as outlined above and by the adiabatic scheme described in Ref. [11]. Both start from an initial spin-coherent state $|\psi_0\rangle = |m_y = -3\rangle$, which has equal uncertainties for the components ΔF_x and ΔF_z . This state is a good approximation to the ground state of the control Hamiltonian when the magnetic field $\mathbf{B}(t) = B(t)\mathbf{y}$ and $B(t)$ is large. As the field magnitude is slowly reduced

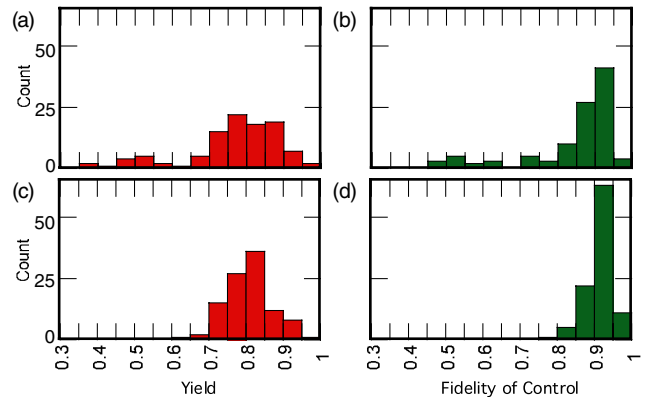


FIG. 3 (color online). Histograms of (a) yields and (b) fidelities of measured vs predicted states. (c),(d) Yields and fidelities when each measured state is geometrically rotated to optimize fidelity relative to the predicted state.

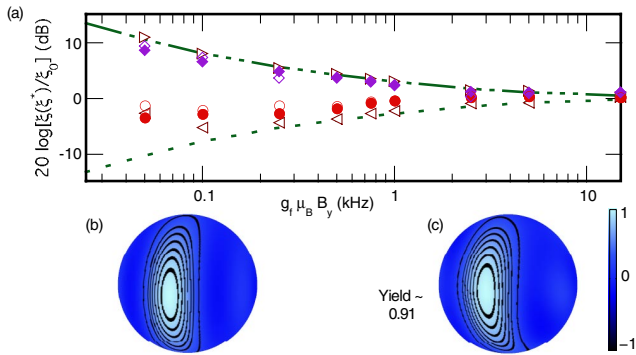


FIG. 4 (color online). Spin squeezing by adiabatic control. (a) Normalized squeezing parameter vs final magnetic field for the squeezed and antisqueezed components. Dashed lines: Perfect squeezing. Open triangles: Full model predictions for adiabatic control. Solid circles and diamonds: Experimental results for adiabatic control. Open circles and diamonds: Experimental results for optimal control. (b) Target and (c) measured Wigner functions corresponding to the smallest observed ξ .

over ~ 1 ms, the state adiabatically evolves to minimize the squeezing parameter $\xi = \Delta F_x / |\langle F_y \rangle|$ of relevance for metrology [19]. Figure 4(a) shows the squeezing and anti-squeezing that results as $B(t)$ is ramped to different final values, relative to a spin-coherent state with the same $|\langle F_y \rangle|$. Up to ~ 4 dB of squeezing is seen in the experiment, in good agreement with model predictions. For the small spin used here, the squeezing is quickly limited by the decrease in $|\langle F_y \rangle|$ as the squeezing ellipse wraps around the sphere. Figures 4(b) and 4(c) show Wigner functions for the target and the actual state for the smallest ξ achieved in our experiment ($\sim 80\%$ of the coherent state value). We have produced the same spin-squeezed states via optimal control, with small but significant reductions in both squeezing and yield. This is most likely because adiabatic control is inherently robust against control errors and thus advantageous even in the presence of extra decoherence during the longer control waveforms.

In conclusion, we have implemented a scheme for optimal control of the spin of a Cs atom in the $F = 3$ ground state. Control Hamiltonians were designed to produce a range of target states, applied in the laboratory, and evaluated by measuring the resulting density matrices. Typical yields fall in the range 0.8–0.9. Among the targets were a number of spin-squeezed states, which allowed comparison of optimal control to an adiabatic squeezing scheme robust to control errors. In future experiments, we plan to use a combination of rf and microwave fields to control the entire 16-dimensional state space for the Cs $6S_{1/2}(F = 3, 4)$ ground manifold. Preliminary studies indicate that this system is fully controllable on a time scale of a few tens of microseconds with easily available control fields. This will provide an important tool for the encoding and manipulation of qubits and qudits embedded in a larger

atomic ground manifold. An example is magnetic field insensitive encodings $|F, m\rangle$, $|F + 1, -m\rangle$, where the qubit states are not easily coupled by one-photon microwave or two-photon optical Raman transitions if $m \neq 0$ [20]. It is also interesting to consider if control Hamiltonians of the form used here can be achieved for collective spins, for example, through coherent optical feedback [21] or through atom-atom interactions in a quantum-degenerate gas [22].

This research was supported by NSF Grants No. PHY-0355073 and No. PHY-0355040, ONR Grant No. N00014-05-1-420, and DTO Grant No. DAAD19-13-R-0011.

-
- [1] L. M. K. Vandersypen and I. L. Chuang, *Rev. Mod. Phys.* **76**, 1037 (2004).
 - [2] P. W. Brumer and M. Shapiro, *Principles of the Quantum Control of Molecular Processes* (Wiley InterScience, Hoboken, NJ, 2003); H. Rabitz *et al.*, *Science* **288**, 824 (2000).
 - [3] M. A. Nielsen and I. L. Chuang, *Quantum Computation and Quantum Information* (Cambridge University Press, Cambridge, England, 2000).
 - [4] V. Giovannetti, S. Lloyd, and L. Maccone, *Science* **306**, 1330 (2004).
 - [5] H. A. Rabitz, M. M. Hsieh, and C. M. Rosenthal, *Science* **303**, 1998 (2004).
 - [6] I. Walmsley and H. Rabitz, *Phys. Today* **56**, No. 8, 43 (2003).
 - [7] V. Ramakrishna *et al.*, *Phys. Rev. A* **51**, 960 (1995).
 - [8] J. S. Li and N. Khaneja, *Phys. Rev. A* **73**, 030302(R) (2006).
 - [9] A. C. Doherty *et al.*, *Phys. Rev. A* **62**, 012105 (2000).
 - [10] A. Silberfarb, P. S. Jessen, and I. H. Deutsch, *Phys. Rev. Lett.* **95**, 030402 (2005); G. A. Smith *et al.*, *ibid.* **97**, 180403 (2006).
 - [11] A. S. Sørensen and K. Mølmer, *Phys. Rev. Lett.* **86**, 4431 (2001).
 - [12] See, for example, P. S. Jessen, I. H. Deutsch, and R. Stock, *Quant. Info. Proc.* **3**, 91 (2004), and references therein.
 - [13] G. K. Brennen, D. P. O’Leary, and Stephen S. Bullock, *Phys. Rev. A* **71**, 052318 (2005).
 - [14] J. M. Geremia, J. K. Stockton, and H. Mabuchi, *Phys. Rev. Lett.* **94**, 203002 (2005).
 - [15] J. M. Geremia, J. K. Stockton, and H. Mabuchi, *Phys. Rev. A* **73**, 042112 (2006); I. H. Deutsch and P. S. Jessen (unpublished).
 - [16] G. A. Smith *et al.*, *Phys. Rev. Lett.* **93**, 163602 (2004).
 - [17] P. Giorda, P. Zanardi, and S. Lloyd, *Phys. Rev. A* **68**, 062320 (2003).
 - [18] J. P. Dowling, G. S. Agarwal, and W. P. Schleich, *Phys. Rev. A* **49**, 4101 (1994).
 - [19] D. J. Wineland *et al.*, *Phys. Rev. A* **50**, 67 (1994).
 - [20] For a discussion of universal control by optical Raman transitions, see [13].
 - [21] M. Takeuchi *et al.*, *Phys. Rev. Lett.* **94**, 023003 (2005).
 - [22] A. Micheli *et al.*, *Phys. Rev. A* **67**, 013607 (2003).